Biochemistry and Biophysics Reports 23 (2020) 100774

Contents lists available at ScienceDirect

Biochemistry and Biophysics Reports

journal homepage: www.elsevier.com/locate/bbrep

Structural features and oligomeric nature of human podocin domain

Sandeep K.N. Mulukala [a], Shivkumar S. Irukuvajjula [b], Krishan Kumar [c], Kanchan Garai [d], Pannuru Venkatesu [c], Ramakrishna Vadrevu [b], Anil K. Pasupulati [a,*]

[a] Department of Biochemistry, School of Life Sciences, University of Hyderabad, Hyderabad, 500046, India
[b] Department of Biological Sciences, Birla Institute of Technology and Sciences, Pilani Hyderabad Campus, Hyderabad, 500078, India
[c] Department of Chemistry, University of Delhi, New Delhi, 110 007, India
[d] Tata Institute of Fundamental Research, Hyderabad, 500019, India

ARTICLE INFO

Keywords:
Podocin
Podocyte
Nephrotic syndrome
Slit-diaphragm
Proteinuria

ABSTRACT

Podocytes are crucial cells of the glomerular filtration unit and plays a vital role at the interface of the blood-urine barrier. Podocyte slit-diaphragm is a modified tight junction that facilitates size and charge-dependent permselectivity. Several proteins including podocin, nephrin, CD2AP, and TRPC6 form a macromolecular assembly and constitute the slit-diaphragm. Podocin is an integral membrane protein attached to the inner membrane of the podocyte via a short transmembrane region (101–125). The cytosolic N- and C-terminus help podocin to attain a hook-like structure. Podocin shares 44% homology with stomatin family proteins and similar to the stomatin proteins, podocin was shown to associate into higher-order oligomers at the site of slit-diaphragm. However, the stoichiometry of the homo-oligomers and how it partakes in the macromolecular assemblies with other slit-diaphragm proteins remains elusive. Here we investigated the oligomeric propensity of a truncated podocin construct (residues:126–350). We show that the podocin domain majorly homo-oligomerizes into a 16-mer. Circular dichroism and fluorescence spectroscopy suggest that the 16-mer oligomer has considerable secondary structure and moderate tertiary packing.

1. Introduction

Vertebrate kidneys regulate electrolyte and water balance to maintain body homeostasis. Each kidney is composed of about one million nephrons. The glomerulus and the renal tubule are the two major parts of a nephron that work in unison to ensure ultra-filtrated urine. The glomerular filtration barrier (GFB) offers permselectivity for the filtration of plasma components into the urine. The GFB consists of fenestrated capillary endothelium, glomerular basement membrane, and podocytes [1]. Podocytes are highly differentiated visceral epithelial cells that encase the glomerular capillaries. A typical podocyte cell consists of a protuberant cell body with primary processes made of actin and microtubules. The primary process further branches into secondary foot processes which interlaces with the neighboring foot processes forming a modified tight junction called the slit-diaphragm (SD) [2]. The SD is a negatively charged zipper-like structure bridging the 30–40nm gap between the adjacent foot processes. This structure curbs the passage of albumin and other large molecules from the blood into primary urine thereby tightly regulating the composition of the glomerular filtrate [3,4]. The intricate structure of the SD is maintained by an array of protein assemblies. Proteins such as podocin, nephrin, CD-2 associated protein (CD2AP), transient receptor potential cation channel subfamily C- member 6 (TRPC6), zonula occludens-1 (ZO-1), and Nephrin-like proteins 1, 2, and 3 (NEPH) interact to form macromolecular complexes and constitute the structure of SD [5–8].

Mutations in the SD proteins are associated with nephrotic syndrome (NS), which is presented with massive proteinuria, hypoalbuminemia, and edema [9]. Corticoid therapy is the usual recourse to abate NS and based on the patient's response to corticoid therapy NS is divided into steroid-sensitive NS (SSNS) and steroid-resistant NS (SRNS). Patients with congenital nephropathies usually belong to the SRNS group since they do not respond to corticoid therapy. Congenital nephropathy typically onsets in infants during 0–3 months of age which eventually progresses to irreversible kidney failure within a decade. Mutations in

Abbreviations: SD, slit-diaphragm; GFB, Glomerular filtration barrier; CD2AP, CD-2 associated protein; TRPC6, Transient receptor potential cation channel subfamily C member 6; ZO-1, Zonula occludens-1; NEPH, Nephrin-like protein; NS, Nephrotic syndrome; SRNS, steroid-resistant NS; *NPHS1* & 2, Nephrotic syndrome-type I and type II; IDRs, Intrinsically disordered regions; SEC, Size-exclusion chromatography; MALS, multi-angle light scattering; CD, Circular dichroism.

* Corresponding author. F73B, School of Life Sciences, University of Hyderabad, Gachibowli, Hyderabad, 500046, India.
E-mail address: pasupulati.anilkumar@gmail.com (A.K. Pasupulati).

https://doi.org/10.1016/j.bbrep.2020.100774
Received 15 April 2020; Received in revised form 31 May 2020; Accepted 2 June 2020

NPHS1 and *NPHS2* that encode for nephrin and podocin respectively result in the majority of congenital SRNS cases [10]. About 18% of the reported SRNS cases are due to mutations in podocin [11,12]. Mutations in other SD proteins such as TRPC6 and CD2AP have also been observed to cause NS but at a less frequent rate than nephrin and podocin [13–15].

Podocin is a 383 amino acid protein localizing to the lipid rafts along with other SD proteins [7,16,17]. Podocin shares 44% homology and several structural similarities with stomatin family proteins due to the presence of a highly conserved Prohibitin (PHB) domain [5,18]. Podocin adapts a hook-like structure with its cytoplasmic N- and C- terminus as it attaches to the inner side of the plasma membrane via a transmembrane domain at 100–125 residues [5,12,19]. Structural characterization of stomatin revealed that different truncations of the protein associated with different oligomeric states and the C-terminus of the protein is crucial for homo-oligomerization [20–22]. Studies with truncated C-terminal human podocin revealed that it forms a dimer [23]. Though it was proposed that longer constructs of podocin were capable of associating into higher-order oligomers, it was never demonstrated [23]. Additionally, co-immunoprecipitation studies with nephrin, CD2AP, TRPC6, and NEPH1 indicated that these proteins interact majorly with the C-terminus of podocin [6–9,16,17,24]. We reported earlier that these interactions are mediated by the intrinsically disordered regions (IDRs) present in these proteins [18].

Although a large body of evidence suggests a central role for the podocin in the SD protein complex, the precise mechanism by which podocin oligomerizes and acts as a scaffolding molecule remains to be elucidated. Importantly, it is not known whether all the other SD proteins interact with a single podocin or with homo-oligomers? Therefore, in this study, we attempted to understand the oligomeric nature of protein using a truncated construct (residues: 126–350), which encompasses the PHB domain, C-terminal oligomerization site, and 4 out of the 6 cysteines present in the native podocin sequence.

2. Material and methods

2.1. Protein cloning, expression, and purification

The codon-optimized podocin gene (1152bp) was purchased from Gene Art (Life Technologies, USA). The regions encoding the amino acids 126–350 (podocin domain) was amplified with the primers 5′ CCC GAA TTC G AAA GTG GTG CAA GAA 3’ (forward) and 5′ GAA CTC GAG CAG ACA ATT CAG CAG ATC 3’ (reverse) and cloned into pET22b at EcoRI/XhoI sites. The recombinant construct was transformed into Arctic express (DE3) competent cells (Agilent Technologies, USA). The transformed cells were grown at 37 °C in LB media supplemented with 100 μg/ml ampicillin and 10 μg/ml gentamycin. Protein expression was induced with 0.2 mM IPTG and cultured further for 16hrs at 14 °C. The cells were harvested by centrifugation (13300×*g*, 20 min, and 4 °C) and sonicated in the opening buffer (50 mM potassium phosphate (pH 8.0), 0.3 M NaCl, 5 mM β-mercaptoethanol and 0.1% Triton X-100) followed by clarification by centrifugation at 18000×*g* for 45 min at 4 °C. The inclusion bodies were solubilized in 50 mM potassium phosphate (pH 8.0), 0.3 M NaCl, 5 mM β-mercaptoethanol and 8 M Urea followed by clarification at 18000×*g* for 1h at room temperature. The solubilized protein was then purified using Ni-NTA agarose (Qiagen). The purity was confirmed (>98%) on a 12% SDS-PAGE. From the SDS-PAGE gel, the band corresponding to the podocin domain (27 kDa) was excised and subjected to tryptic digestion and analyzed using MALDI-TOF/TOF (Bruker Autoflex III smart beam, Bruker Daltonics, Bremen, Germany) to confirm the protein sequence.

The purified protein was renatured by rapid dilution at 1:10 into 10mM potassium phosphate buffer with 150 mM NaCl and 2 mM β-mercaptoethanol (pH 8.0) followed by dialysis in the same buffer to remove traces of urea and imidazole. The same pH and buffer composition are uniformly used in all the subsequent experiments. An extinction coefficient of the 12950 M^{-1} cm^{-1} was used for determining the protein concentration on Jasco V-630 UV–Vis spectrophotometer.

2.2. Size exclusion chromatography and multi-angle light scattering analysis (SEC-MALS)

We performed SEC-MALS to estimate the oligomeric nature of the podocin domain. SEC-MALS was performed at room temperature by passing 500 μl protein (12μM) at 0.3 ml/min flow rate through a Superdex S200 SEC column (GE Healthcare) pre-equilibrated with 10mM potassium phosphate buffer supplemented with 150mM NaCl and 2mM β-mercaptoethanol (pH 8.0). This column was attached to the MALS system (AF2000- Postnova) for analyzing the molar mass of the protein. The protein sample from SEC-MALS was next passed through the flow cell equipped Zetasizer Nano ZS90 dynamic light scattering (DLS) device (Malvern Instruments Ltd, UK) equipped with a 4 mW He–Ne laser. The backscattering was measured at 173 nm for analyzing the polydispersity index (PDI) and the hydrodynamic radius of the protein.

2.3. Fluorescence spectroscopy

Intrinsic tryptophan fluorescence was measured using Jasco FP-6300 (Japan) equipped with an intense xenon flash lamp as the light source. 287 nm was used as the excitation wavelength and the 300–450 nm spectral range was used for obtaining the emission spectrum of the sample (12 μM). For accessing the stability of the podocin domain thermal-induced unfolding was performed. Fluorescence emission at 335 nm as a function of increasing temperature was recorded in triplicates at a bandwidth of 2.5 nm and a scan speed of 200 nm/min for every degree rise in temperature. All the spectra were buffer corrected. The effect of temperature on the protein stability was analyzed by plotting fluorescence intensity at 335 nm using Origin (pro)-version2020b (Origin Lab Corporation, Northampton, MA).

2.4. Circular dichroism (CD) spectroscopy

The CD spectroscopy measurements were recorded on Jasco J-1500 spectropolarimeter (Japan) equipped with a thermoelectric cell holder. The Far-UV (260-195 nm) CD measurements of podocin domain (12 μM) were recorded using a 0.2 cm path length cell at 2.5 nm bandwidth and a scan speed of 50 nm/min. The Near-UV CD measurements were also recorded for the protein sample at 25 μM concentration using a 0.5cm pathlength cell at the bandwidth of 2.5nm and a scan speed of 100 nm/min. Both for far-UV and near-UV the data was recorded in triplicates. To assess the effect of temperature and thus the stability of the domain, the sample was subjected to a steady increase in temperature, and spectra were recorded at an interval of 5 °C over a spectral range of 200 nm–250 nm. The data were plotted using origin lab software after buffer correction.

2.5. Calorimetric analysis

The transition temperature (T_g) of the podocin domain was obtained from measurements using NANO DSC (TA Instruments, USA). Sample containing protein concentration of 12 μM and a volume of 0.650 μL was loaded into the sample capillary and change in heat flow was recorded against reference buffer at a constant pressure of 3 atm, over a temperature range of 293 K–368 K, with a scan rate of 1 K/min and a 300-sec cell equilibration time. Buffer scans were first performed before loading protein for baseline reproducibility. The obtained data was buffer corrected and the analysis data was plotted for peak integration with the peak analyzer option in Origin pro 2020b software. From the peaks, the T_g and the enthalpy of transition (ΔH_{cal}) were calculated.

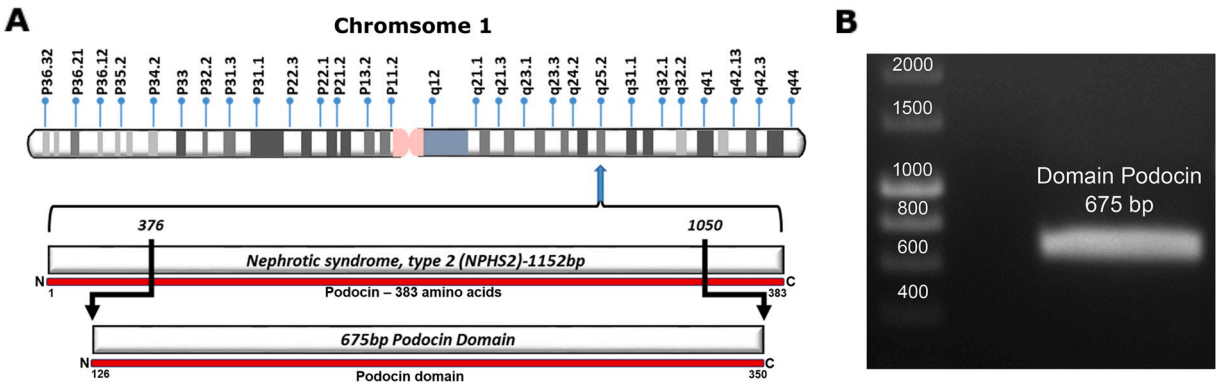

Fig. 1. Cloning of podocin domain: A. The NPHS2 gene that encodes podocin is located on chromosome 1 at the locus q25.2. B. The region 376bp – 1050bp of the gene was amplified and cloned into pET22b bacterial expression vector.

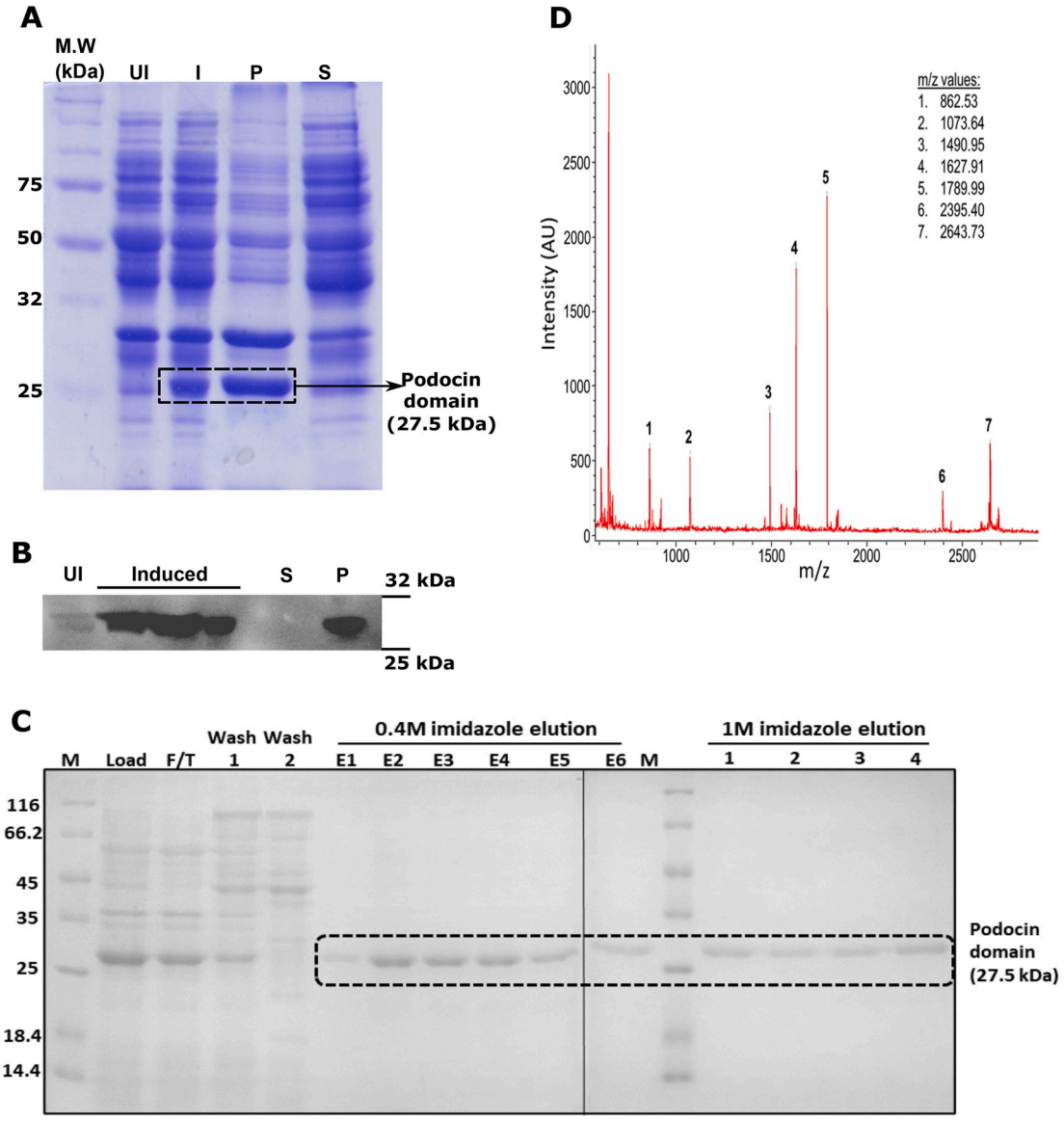

Fig. 2. Expression, and purification of podocin domain: A & B. Coomassie blue staining and immunoblotting with His-Tag HRP-conjugated antibody were done to identify the expression and solubility of the podocin domain. C. The SDS-PAGE analysis of samples after affinity chromatography purification of the urea solubilized cell lysate. D. Trypsinization and MALDI-TOF/TOF analysis of the 27KDa band excised from the earlier SDS-PAGE gel confirmed the presence of the podocin domain. UI-uninduced culture, I-Isopropyl β, D - thiogalactopyranoside Induced culture, P-Pellet fraction, S-Soluble fraction, F/T-flow through, E1-E6: elution fractions with 0.4 M imidazole, 1–4: elution fractions with 1 M imidazole. (For interpretation of the references to color in this figure legend, the reader is referred to the Web version of this article.)

Table 1
MALDI TOF/TOF analysis of the purified protein: Trypsinization of the purified band at 27 kDa and subsequence analysis by MALDI-TOF/TOF showed 5 peptide sequences. BLAST analysis of these sequences against the non-redundant proteins database of NCBI showed 100% similarity with the human podocin sequence. Note: The black trinagle indicates the site of digestion by trypsin at arginine and lysine residues in the sequence.

Sequence		Observed	Mr (expt.)	Mr (calc.)	Expect	Peptide
Start	End					
134	146	1490.95	1489.95	1489.93	2.3e-03	R▲VIIFRLGHLLPGR▼A
149	168	2395.40	2394.40	2394.22	9.1e-03	K▲GPGLFFFLPCLDTYHKVDLR▼L
263	286	2643.73	2642.72	2642.45	6.1e-04	R▲IEIKDVRLPAGLQHSLAVEAEAQR▼Q
270	286	1789.99	1788.99	1788.95	2.4e-06	R▲LPAGLQHSLAVEAEAQR▼Q
307	322	1627.91	1626.90	1626.88	3.5e-06	R▲MAAEILSGTPAAVQLR▼Y

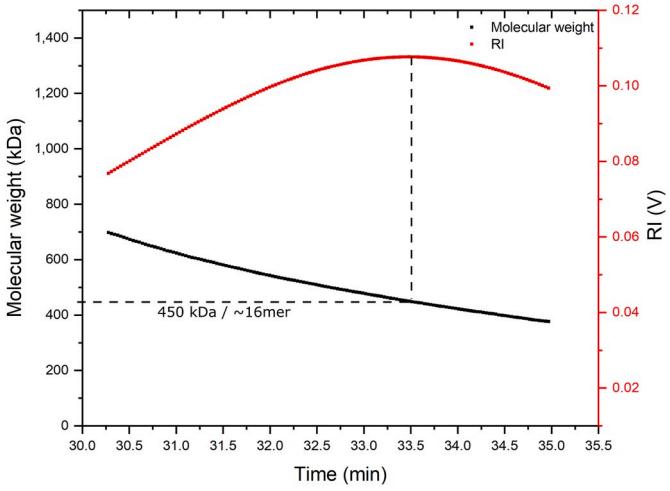

Fig. 3. Podocin domain forms higher-order oligomers: SEC-MALS analysis of the podocin domain for molecular mass determination. The molecular weight on Y-axis and the refractive index on the secondary axis and were plotted against elution time.

3. Results

3.1. Purification of podocin domain

The region from 376bp to 1050bp of human *NPHS2* gene encoding 126–350 amino acid residues of podocin was PCR amplified and cloned into the pET22b expression vector (Fig. 1A&B). IPTG induced expression of the construct resulted in the protein to form inclusion bodies which were confirmed by Coomassie blue staining and immunoblotting with anti-His antibody (Fig. 2A&B). The protein was purified from inclusion bodies by Ni-NTA affinity chromatography after solubilization in 8 M urea (Fig. 2C). Tryptic digestion of the band corresponding to the podocin domain from the SDS-PAGE gel (Fig. 2C-lane E2) and subsequent analysis of the digested products by MALDI-TOF/TOF revealed five peptide fragments (Fig. 2D and Table 1). NCBI BLAST search of these peptide sequences against the non-redundant database confirmed the purified protein as human podocin covering the region 126–350 amino acids.

3.2. Oligomeric nature of the podocin domain

It was reported that stomatin family members exist as homo-oligomers [20–22]. Since podocin shares significant homology with stomatin, we analyzed the oligomeric nature of the podocin which includes the PHB domain. SEC-MALS data is represented as a combinatorial plot of refractive index, and molecular weight versus elution time (Fig. 3). A maximum refractive index value of 0.11 was observed which corresponds to a molecular weight of 450kDa, suggesting that the podocin domain is a 16-mer oligomer (monomer = 27.5kDa; therefore; 450 kDa/27.5 kDa = ~16-mer). In addition to the predominant 16-mer species, other oligomeric conformations of the podocin domain ranging from 25-mer (refractive index: 0.08, molecular weight: 697kDa) to 13-mer (refractive index: 0.10, molecular weight: 376kDa) were also observed, but to a lesser extent. The DLS, which was in tandem with the SEC-MALS analyzed the eluted samples for hydrodynamic radius and polydispersity. A hydrodynamic radius range of 13.39 - 9.37 nm corresponding to elutions from 25-mer to 13-mer was observed respectively (Fig. 4A–E). The average PDI of the sample was found to be 0.14, which suggests that the sample consists of one major population by volume, however, a broad size range within the population implies the presence of different size species. From these results, it is evident that the major species the podocin domain is a 16-mer while a minor population of other higher-order oligomers also appears to exist in solution.

3.3. Structural features of the homo-oligomers of podocin domain

The CD spectra in the far UV region (250-195 nm) provides information on the secondary structure while the near UV region (310-250 nm) on the tertiary packing. The far UV CD signal for the truncated podocin domain indicates that the protein adopts secondary structure (Fig. 5A). The shape of the spectrum suggests the presence of both α−helices and β−sheet structures. The near UV spectrum of the sample shows a broad peak at 280nm typically contributed by the tryptophan residue (W256), and a minor peak from ~250 – 260 nm could be contributed by five-tyrosine and eight-phenylalanine residues (Fig. 5B). The CD data in the near UV regions suggests the arrangement of aromatic amino acids in a restricted environment and thus implying a folded structure adopted by the polypeptide chain. The intrinsic tryptophan emission spectrum of the podocin domain shows λ_{max} value at 335 nm (Fig. 5C). The λ_{max} of native proteins is related to the polarity of the environment of the tryptophan residue and typically can range from 308-350 nm. Unfolded forms with residues in the apolar microenvironment show a blue shift of the λ_{max} [25].

3.4. Structural stability of the podocin domain

Although, the intrinsic fluorescence may not unequivocally provide

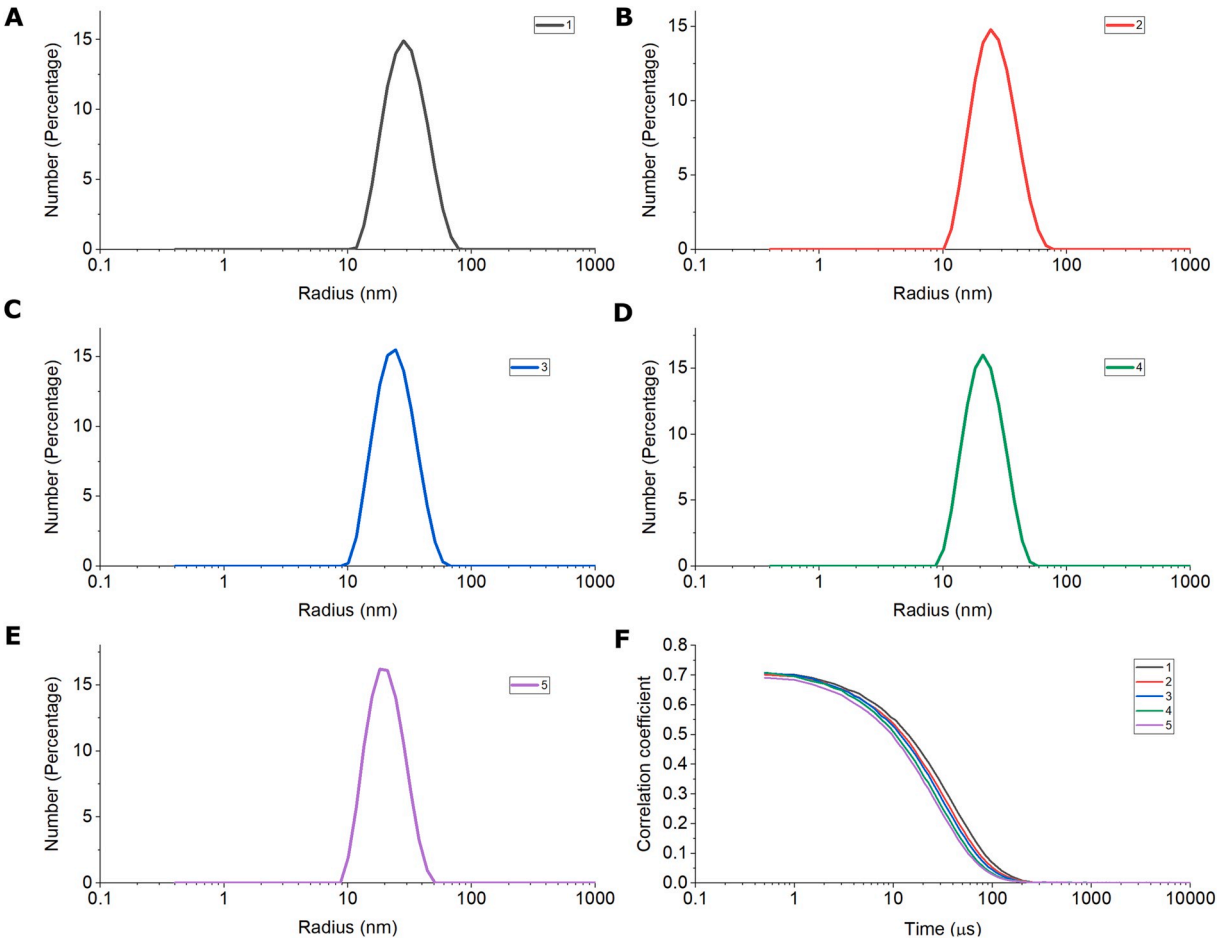

Fig. 4. Polydispersity and hydrodynamic radius of the podocin domain homo-oligomers: The DLS was in tandem with the SEC-MALS. DLS analysis of the samples corresponding to peak observed in SEC-MALS (1–5) is represented as a number percentage vs size in nanometers curve plots marked in different colors (A–E). The corresponding correlograms of the samples (1–5) represented as correlation coefficient vs time in microseconds. (For interpretation of the references to color in this figure legend, the reader is referred to the Web version of this article.)

structural information, the changes in the folded state can be followed by monitoring the emission intensity which conveys the changes in the native state tryptophan environment. The changes in the CD signal and the perturbations of the intensity of the intrinsic fluorescence emission were estimated to assess the stability of the folded podocin domain. Temperature-induced unfolding was monitored using the fluorescence emission spectra with increasing temperature in the range of 20 °C–95 °C. The spectra showed a uniform decrease in λ_{max} intensity without either a bathochromic or hypsochromic shift (Fig. 6A). The change in fluorescence intensity as a function of temperature (Fig. 6B) shows a linear transition and does not show a sigmoidal shape typically observed for proteins with a tightly packed tertiary core. The absence of a folded baseline suggests a not so tightly packed tertiary core. Far UV CD spectral changes were also monitored as a function of temperature. With the gradual increase in temperature a gradual loss of signal intensity (Fig. 6C), loss of secondary structure, and also the absence of a native baseline was observed (Fig. 6D) implying that the podocin domain possesses secondary and tertiary interactions but lack a tightly packed core.

3.5. Calorimetric analysis of podocin domain

Differential scanning calorimetry (DSC) gives the overall enthalpy value (ΔH_{cal}) for each structural transition. Therefore, we performed DSC to calculate the thermodynamic parameters such as T_g and the ΔH_{cal} associated with structural changes of the homo-oligomer. Peak deconvolution of the acquired data revealed 5 transition states, out of which four are endothermic transitions (316 K, 325 K, 330 K, and 353 K) and one is an exothermic transition (345 K) (Fig. 7). The respective values for ΔH_{cal} are mentioned in Table 2. The DSC profile suggests that the oligomers in the mixture undergo dissociation via three transition temperatures namely 316 K, 325 K, and 330 K and the presence of exothermic transition at 345 K suggests possible hydrophobic interactions among the constituent oligomers before complete dissociation at 353 K.

4. Discussion

Podocin selectively expresses in the glomerular podocytes and it is instrumental for preserving the structural integrity of the SD. Though several mutations in the protein are associated with proteinuria in humans, the structural details of this protein are unclear. Here we report for the first time, the stoichiometry of oligomerization of the truncated human podocin construct. Our investigation indicates that at ambient temperature, and in a reduced environment the podocin domain predominantly adopts a 16-mer oligomeric state. However, other oligomeric conformations ranging from 25-mer to 13-mer were also observed nevertheless, the population of these states was comparatively less. The polydispersity index we report adds evidence to the presence of multiple oligomeric species. Additionally, CD and fluorescence spectra revealed podocin homo-oligomers have considerable secondary structure and tertiary packing.

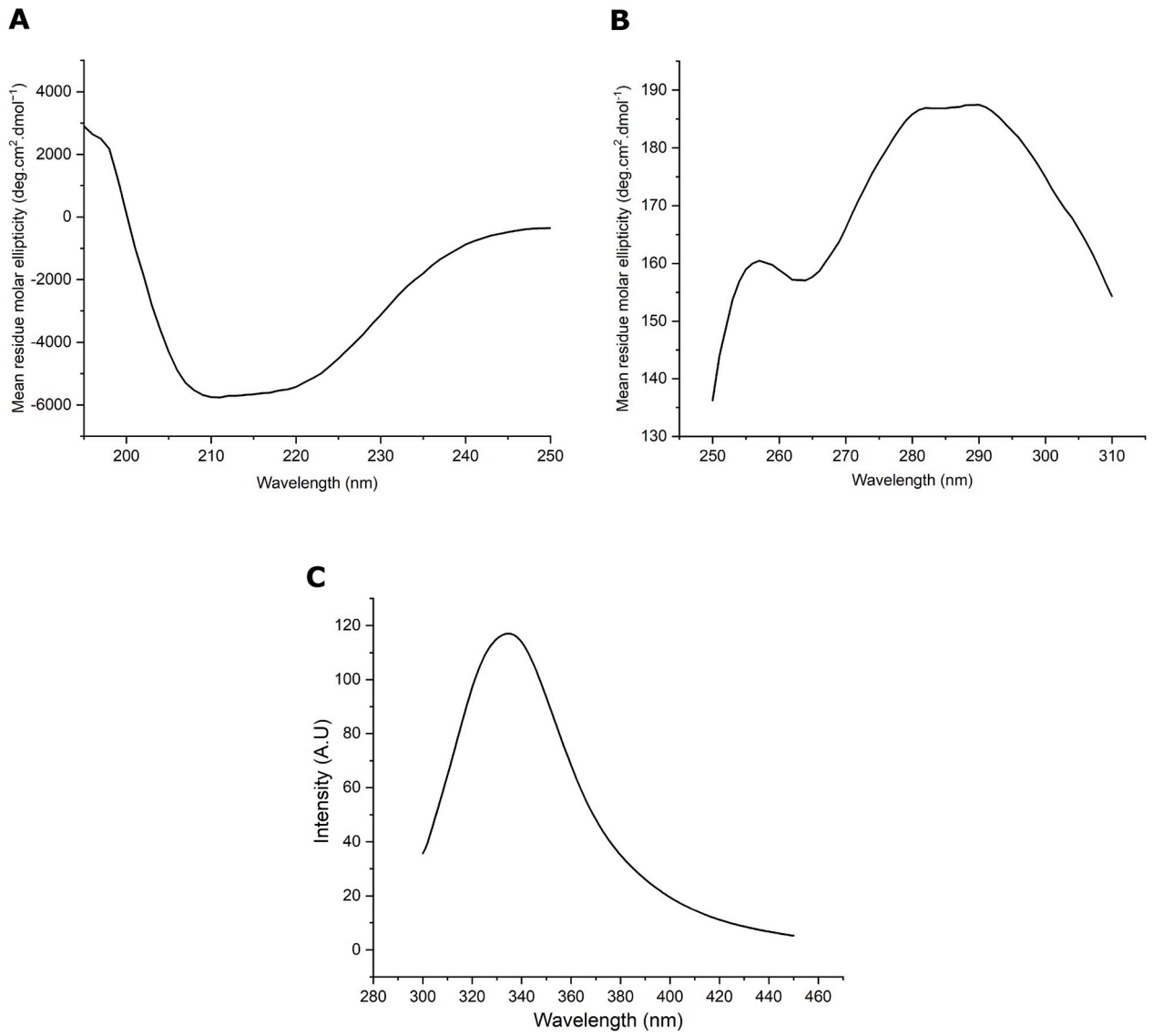

Fig. 5. Podocin domain exhibits secondary structural elements and tertiary packing: A. Far-UV CD spectrum of Podocin domain at 25 °C, pH 8 in 10mM potassium phosphate buffer supplemented with 150mM NaCl and 2mM β-mercaptoethanol. B. Near-UV CD spectrum representing the tertiary packing of the podocin domain. C. Fluorescence emission of the podocin domain recorded by exciting the protein at 287 nm.

Since stomatin proteins and podocin share significant homology, it expected they may share several structural similarities. Crystallization studies of stomatin protein (*Pyrococcus horikoshii*; residues 56–224) revealed that it exists as a trimer and NMR studies of the same protein with a different truncation size (residues 66–174) associated into an amalgam of oligomers [20]. Although earlier reports suggested that podocin forms homo-oligomers the specificity of oligomerization was not known [7,16,17,26]. Even though our study revealed truncated podocin forms predominantly a 16-mer, we are yet to demonstrate whether full-length podocin also assembles as a 16-mer which is a major limitation of our study. We were unsuccessful in purifying the full-length podocin that could be due to several reasons including podocin may not be stable outside its native environment, due to the presence of IDRs, or interference of the transmembrane segment with protein expression [5]. We, therefore, performed our studies with truncated podocin (126–350 residues) that encompasses the PHB domain and the oligomerization sites. The regions '283–313' and '332–348' of podocin facilitate intermolecular interactions [23]. Huber et. al, reported that podocin (R138X) was unable to form oligomers suggesting the importance of this region in podocin-podocin interactions [17]. We included the 126–164 residues upstream of the PHB domain as it was reported that the high-affinity binding among homo-oligomers requires larger parts of the C-terminal region besides the PHB domain [17]. Accumulating evidence suggests that 126–350 region of podocin is crucial for homo-oligomerization, it can be expected that mutations in these regions likely distort the intermolecular interactions. Mutations that cause NS could distort the innate ability of podocin to form oligomers and compromise its ability to act as a scaffolding molecule. Together these molecular deformations at the level of podocin oligomeric assembly may lead to altered permselectivity of SD and manifest in significant proteinuria. As it was shown that podocin interacts with several SD proteins, it is less likely a single podocin interacts with all proteins whereas a different monomer of the podocin 16-mer may interact with the neighboring proteins in the SD complex. It should be noted that the podocin domain predominantly forms a 16-mer, and to a lesser extent 25-mer to 13-mer are also observed. These results are further justified by the hydrodynamic radius and the polydispersity index (PDI) measured by the DLS. The reported PDI for podocin domain falls in the midrange value (0.08–0.5) suggesting that although it has one major oligomer species by volume, the presence of multiple species could be possible [27]. We were unable to

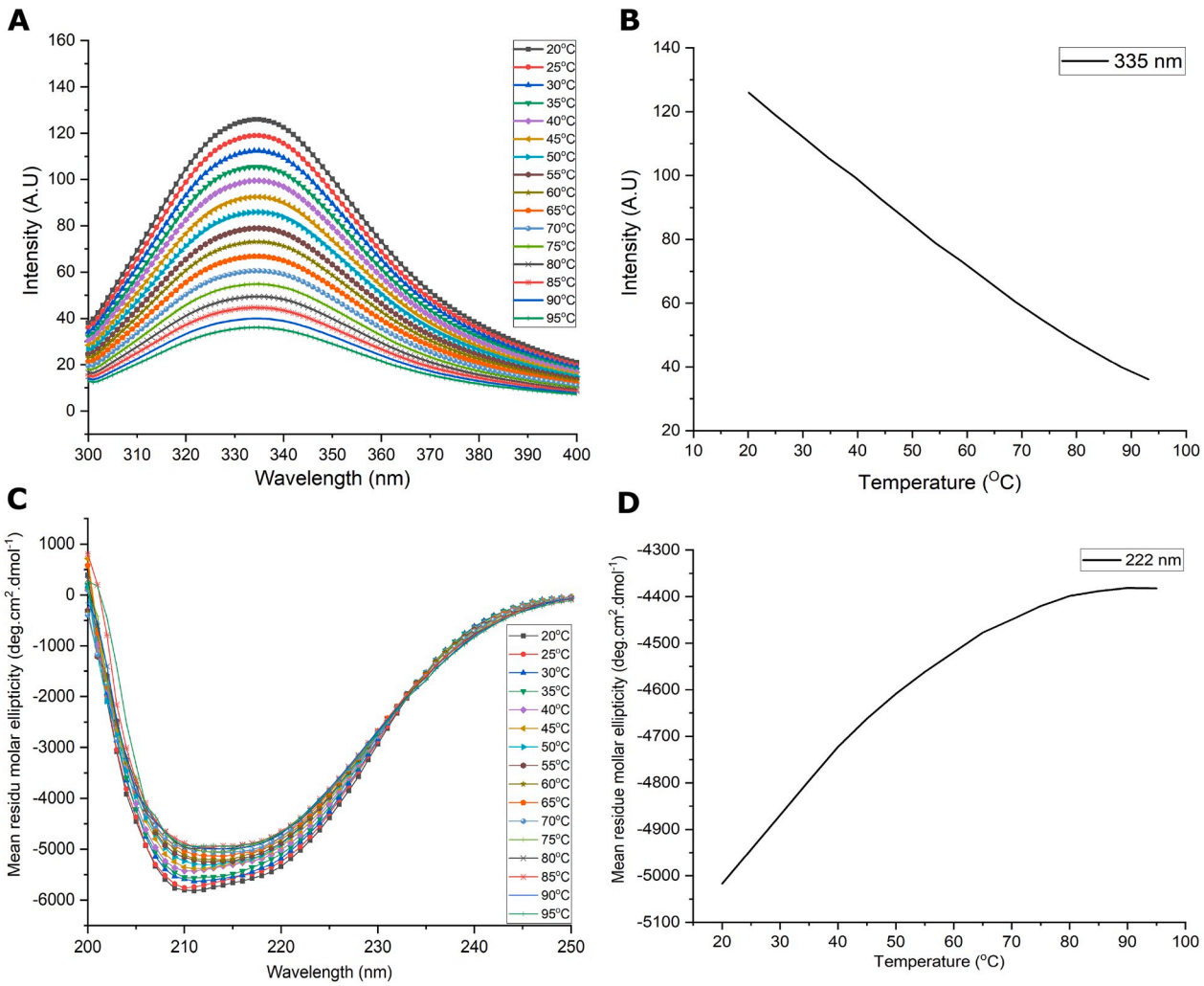

Fig. 6. Effect of temperature on podocin domain: A. Intrinsic tryptophan fluorescence for podocin domain was measured as a function of temperature (20 °C–95 °C) by exciting the protein at 287 nm. B. Peak emission of the podocin domain at 335 nm is plotted over a temperature range of 20 °C–95 °C. C. FarUV CD spectra (250–200 nm) of the podocin domain was acquired as a function of temperature (20 °C–95 °C). D. The MRE values of the podocin domain at 222nm is plotted as a function of temperature (range: 20 °C–95 °C) to monitor the changes in the protein structure.

obtain crystals of the podocin domain for performing X-ray diffraction possibly due to its dynamic oligomeric nature.

Far UV-CD spectra revealed that the podocin domain consists of a considerable amount of α-helices and β-sheets. We could not record far UV-CD spectra beyond 195nm possibly because of the presence of buffer components like β-mercaptoethanol that manifested in increased HT voltage. However, β-mercaptoethanol in the buffer helped in solubilizing podocin domain and contributed towards the protein stability. It is noteworthy that crystal structures of stomatin protein are devoid of disulfide linkages [22,28]. In a study, Huber et.al reported that Cys126 and Cys160 residues of mouse podocin undergo palmitoylation and participate in membrane insertion [26]. Similarly, the Cys158 in the human podocin domain is also expected to be palmitoylated instead of forming disulfide linkages. This suggests that the disulfide bridges between cysteines either do not exist or are not contributing to protein stability.

While assessing the effect of temperature on the protein by probing its intrinsic tryptophan fluorescence and secondary structure content via measuring optical rotation by using the CD, the baseline was observed only in the case of the CD spectrum beyond 80 °C. A significant linear decrease in the fluorescence intensity at 335 nm with increasing temperature may be due to the partial exposure of the lone Trp256 and other aromatic residues as observed in the predicted model for podocin and the crystal structure of stomatin protein (3BK6) (Fig. S1) [18,22]. Also, there was no bathochromic shift observed, which ascertains the fact that the oligomer might not have dissociated completely. Similarly, far UV-CD spectra at 222nm were used to monitor secondary structural changes. A small yet noticeable change in the MRE value and the shape of the spectra implicates that most of the secondary structure was retained, however, a slight rearrangement of structure could be possible, owing to the increased hydrophobic effect. With the increasing temperature, the prominent double minima smoothen out indicating that there might be a slight increase in the β-sheet content. The stable MRE value observed beyond 80 °C might suggest some residual local ordering that still prevails at high temperatures.

Calorimetric analysis of the oligomeric species revealed multiple transition points for the podocin domain. At 20 °C the protein was shown to attain an amalgam of oligomeric states and a steady increase in temperature may promote dissociation of these different oligomers via three different transition temperatures since each oligomeric state may not have same transition point. Nevertheless, when the temperature was further increased significant exothermic transition state was observed. We assume the exothermic transition state may be due to the association of hydrophobic cores of the constituent oligomers. It is well known that lower temperatures do not favor hydrophobic interactions whereas, an increase in temperature to a certain degree promotes hydrophobic

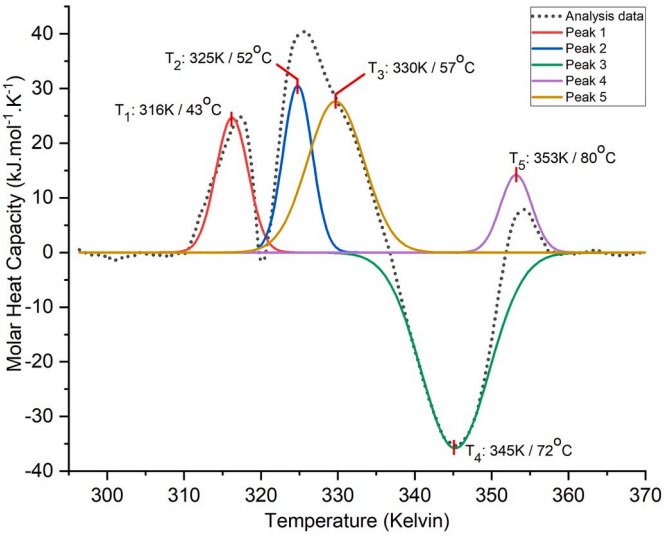

Fig. 7. DSC analysis of podocin domain: The plots represent the endothermic and exothermic transitions of the podocin domain over a temperature range from 296 K/23 °C to 368 K/95 °C. The initial DSC artifact near 293 K/20 °C in the DSC data is not represented in the plot. The analysis data represented as a dotted line in the plot after baseline subtraction. Each transition peak (1–5) in the plot is represented by a color line which is a result of peak deconvolution function. (For interpretation of the references to color in this figure legend, the reader is referred to the Web version of this article.)

Table 2
Enthalpy values and the transition temperatures as noticed in the dynamic scanning calorimetry.

Temperature range	Transition temperatures (T_g)		Enthalpy change (ΔH_{cal}) (kJ/mol)
293 K–368 K/(20 °C–95 °C)	Endothermic	316 K/43 °C	130
		325 K/52 °C	145
		330 K/57 °C	73
		353 K/80 °C	254
	Exothermic	345 K/72 °C	-397

interactions among the protein molecules [29]. Subsequently, when the temperature is further increased, we speculate that the oligomer may invariably disassociate into lower oligomeric species. It is noteworthy that the podocin domain did not re-trace the path to its initial state when the protein was cooled. This peculiar behavior of the podocin domain starkly correlates with the oligomeric propensities as observed in the stomatin proteins [20,21]. Further, we performed above-discussed experiments at 5 °C and found that 16-mer seems to be the major conformer at both lower and ambient temperature (Figs. S2–S5). Interestingly in the calorimetric analysis, multiple transition points were not observed which suggest the presence of 16-mer species as the predominant conformer at lower temperatures and that was further confirmed by SEC analysis (Figs. S4–S5).

In conclusion, our study, to the best of our knowledge is the first to report the cloning, expression, and purification of the human podocin domain (126–350). We showed that the podocin domain is majorly a 16-mer homo-oligomer. However, to a lesser extent, the protein is capable of associating into other oligomeric states. CD and FL analysis of the protein indicated that the podocin domain in isolation attains considerable secondary structure and tertiary packing. However, the significance of the podocin oligomerization in the formation of the large macromolecular complex and how a mutation in a podocin monomer will affect its oligomerization status need to be addressed. Further structural characterization of podocin and other slit diaphragm proteins is greatly warranted to understand the mechanism of pathogenesis of the nephrotic syndrome.

Author statement

Sandeep KMN: Conceptualization, Methodology, Visualization, Writing - Reviewing and Editing.
Shivkumar S Irukuvajjula: Methodology & Validation.
Krishan Kumar: Methodology.
Kanchan Garai: Methodology & Validation.
Pannuru Venkatesu: Methodology, Writing - original Draft.
Ramakrishna Vadrevu: Resources, Conceptualization, Formal Analysis, Writing - Reviewing and Editing.
Anil K Pasupulati: Conceptualization, Formal Analysis, Visualization, Supervision, Funding acquisition, Writing - Reviewing and Editing.

Funding

We acknowledge financial assistance from the Indian Council of Medical Research (Grant no: ICMR 2019/905).

Acknowledgments

We thank Dr. Akif, University of Hyderabad, for providing access to the AKTA-Purifier Gel-filtration system. We also acknowledge the Central Analytical laboratory of BITS - Pilani, Hyderabad campus for allowing access to Circular Dichroism Spectrophotometer. MNSK acknowledges ICMR for providing senior research fellowship.

Appendix A. Supplementary data

Supplementary data to this article can be found online at https://doi.org/10.1016/j.bbrep.2020.100774.

References

[1] P. Anil Kumar, G.I. Welsh, M.A. Saleem, R.K. Menon, Molecular and cellular events mediating glomerular podocyte dysfunction and depletion in diabetes mellitus, Front. Endocrinol. 5 (2014) 151.
[2] A. Patari-Sampo, P. Ihalmo, H. Holthofer, Molecular basis of the glomerular filtration: nephrin and the emerging protein complex at the podocyte slit diaphragm, Ann. Med. 38 (2006) 483–492.
[3] D. Mukhi, R. Nishad, R.K. Menon, A.K. Pasupulati, Novel actions of growth hormone in podocytes: implications for diabetic nephropathy, Front. Med. 4 (2017).
[4] R. Rodewald, M.J. Karnovsky, Porous substructure of the glomerular slit diaphragm in the rat and mouse, J. Cell Biol. 60 (1974) 423–433.
[5] S.K. Mulukala, R. Nishad, L.P. Kolligundla, M.A. Saleem, N.P. Prabhu, A. K. Pasupulati, In silico Structural characterization of podocin and assessment of nephrotic syndrome-associated podocin mutants, IUBMB Life 68 (2016) 578–588.
[6] S.E. Dryer, J. Reiser, TRPC6 channels and their binding partners in podocytes: role in glomerular filtration and pathophysiology, Am. J. Physiol. Ren. Physiol. 299 (2010) F689–F701.
[7] K. Schwarz, M. Simons, J. Reiser, M.A. Saleem, C. Faul, W. Kriz, A.S. Shaw, L. B. Holzman, P. Mundel, Podocin, a raft-associated component of the glomerular slit diaphragm, interacts with CD2AP and nephrin, J. Clin. Invest. 108 (2001) 1621–1629.
[8] N.Y. Shih, J. Li, R. Cotran, P. Mundel, J.H. Miner, A.S. Shaw, CD2AP localizes to the slit diaphragm and binds to nephrin via a novel C-terminal domain, Am. J. Pathol. 159 (2001) 2303–2308.
[9] N.S.K. Mulukala, P.P. Kar, R. Vadrevu, A.K. Pasupulati, Intrinsically disordered regions mediate macromolecular assembly of the Slit diaphragm proteins associated with Nephrotic syndrome, Mol. Simulat. 45 (2019) 603–613.
[10] M. Kestila, U. Lenkkeri, M. Mannikko, J. Lamerdin, P. McCready, H. Putaala, V. Ruotsalainen, T. Morita, M. Nissinen, R. Herva, C.E. Kashtan, L. Peltonen, C. Holmberg, A. Olsen, K. Tryggvason, Positionally cloned gene for a novel glomerular protein–nephrin–is mutated in congenital nephrotic syndrome, Mol. Cell 1 (1998) 575–582.
[11] G. Benoit, E. Machuca, C. Antignac, Hereditary nephrotic syndrome: a systematic approach for genetic testing and a review of associated podocyte gene mutations, Pediatr. Nephrol. 25 (2010) 1621–1632.

[12] N. Boute, O. Gribouval, S. Roselli, F. Benessy, H. Lee, A. Fuchshuber, K. Dahan, M. C. Gubler, P. Niaudet, C. Antignac, NPHS2, encoding the glomerular protein podocin, is mutated in autosomal recessive steroid-resistant nephrotic syndrome, Nat. Genet. 24 (2000) 349–354.
[13] C.E. Sadowski, S. Lovric, S. Ashraf, W.L. Pabst, H.Y. Gee, S. Kohl, S. Engelmann, V. Vega-Warner, H. Fang, J. Halbritter, M.J. Somers, W. Tan, S. Shril, I. Fessi, R. P. Lifton, D. Bockenhauer, S. El-Desoky, J.A. Kari, M. Zenker, M.J. Kemper, D. Mueller, H.M. Fathy, N.A. Soliman, S.S. Group, F. Hildebrandt, A single-gene cause in 29.5% of cases of steroid-resistant nephrotic syndrome, J. Am. Soc. Nephrol. : JASN (J. Am. Soc. Nephrol.) 26 (2015) 1279–1289.
[14] M. Gigante, G. Caridi, E. Montemurno, M. Soccio, M. d'Apolito, G. Cerullo, F. Aucella, A. Schirinzi, F. Emma, L. Massella, G. Messina, T. De Palo, E. Ranieri, G. M. Ghiggeri, L. Gesualdo, TRPC6 mutations in children with steroid-resistant nephrotic syndrome and atypical phenotype, Clin. J. Am. Soc. Nephrol. : CJASN 6 (2011) 1626–1634.
[15] M. Gigante, P. Pontrelli, E. Montemurno, L. Roca, F. Aucella, R. Penza, G. Caridi, E. Ranieri, G.M. Ghiggeri, L. Gesualdo, CD2AP Mutations Are Associated with Sporadic Nephrotic Syndrome and Focal Segmental Glomerulosclerosis (FSGS), Nephrology, Dialysis, Transplantation, vol 24, official publication of the European Dialysis and Transplant Association - European Renal Association, 2009, pp. 1858–1864.
[16] T.B. Huber, M. Kottgen, B. Schilling, G. Walz, T. Benzing, Interaction with podocin facilitates nephrin signaling, J. Biol. Chem. 276 (2001) 41543–41546.
[17] T.B. Huber, M. Simons, B. Hartleben, L. Sernetz, M. Schmidts, E. Gundlach, M. A. Saleem, G. Walz, T. Benzing, Molecular basis of the functional podocin-nephrin complex: mutations in the NPHS2 gene disrupt nephrin targeting to lipid raft microdomains, Hum. Mol. Genet. 12 (2003) 3397–3405.
[18] S.K. Mulukala Narasimha, P.P. Kar, R. Vadrevu, A.K. Pasupulati, Intrinsically disordered regions mediate macromolecular assembly of the Slit diaphragm proteins associated with Nephrotic syndrome, Mol. Simulat. 45 (2019) 603–613.
[19] S. Roselli, O. Gribouval, N. Boute, M. Sich, F. Benessy, T. Attie, M.C. Gubler, C. Antignac, Podocin localizes in the kidney to the slit diaphragm area, Am. J. Pathol. 160 (2002) 131–139.
[20] Y. Kuwahara, S. Unzai, T. Nagata, Y. Hiroaki, H. Yokoyama, I. Matsui, T. Ikegami, Y. Fujiyoshi, H. Hiroaki, Unusual thermal disassembly of the SPFH domain oligomer from Pyrococcus horikoshii, Biophys. J. 97 (2009) 2034–2043.
[21] L. Snyers, E. Umlauf, R. Prohaska, Oligomeric nature of the integral membrane protein stomatin, J. Biol. Chem. 273 (1998) 17221–17226.
[22] H. Yokoyama, S. Fujii, I. Matsui, Crystal structure of a core domain of stomatin from Pyrococcus horikoshii Illustrates a novel trimeric and coiled-coil fold, J. Mol. Biol. 376 (2008) 868–878.
[23] P. Straner, E. Balogh, G. Schay, C. Arrondel, A. Miko, G. L'Aune, A. Benmerah, A. Perczel, K.M. D, C. Antignac, G. Mollet, K. Tory, C-terminal oligomerization of podocin mediates interallelic interactions, Biochimica et biophysica acta, Mol. Basis Dis. 1864 (2018) 2448–2457.
[24] T. Palmen, S. Lehtonen, A. Ora, D. Kerjaschki, C. Antignac, E. Lehtonen, H. Holthofer, Interaction of endogenous nephrin and CD2-associated protein in mouse epithelial M-1 cell line, J. Am. Soc. Nephrol. : JASN (J. Am. Soc. Nephrol.) 13 (2002) 1766–1772.
[25] M.R. Eftink, The use of fluorescence methods to monitor unfolding transitions in proteins, Biophys. J. 66 (1994) 482–501.
[26] T.B. Huber, B. Schermer, R.U. Muller, M. Hohne, M. Bartram, A. Calixto, H. Hagmann, C. Reinhardt, F. Koos, K. Kunzelmann, E. Shirokova, D. Krautwurst, C. Harteneck, M. Simons, H. Pavenstadt, D. Kerjaschki, C. Thiele, G. Walz, M. Chalfie, T. Benzing, Podocin and MEC-2 bind cholesterol to regulate the activity of associated ion channels, Proc. Natl. Acad. Sci. U. S. A. 103 (2006) 17079–17086.
[27] Asmawati, W.A.W. Mustapha, S.M. Yusop, M.Y. Maskat, A.F. Shamsuddin, Characteristics of Cinnamaldehyde Nanoemulsion Prepared Using APV-High Pressure Homogenizer and Ultra turrax 1614, 2014, pp. 244–250.
[28] J. Brand, E.S. Smith, D. Schwefel, L. Lapatsina, K. Poole, D. Omerbasic, A. Kozlenkov, J. Behlke, G.R. Lewin, O. Daumke, A stomatin dimer modulates the activity of acid-sensing ion channels, EMBO J. 31 (2012) 3635–3646.
[29] E. van Dijk, A. Hoogeveen, S. Abeln, The hydrophobic temperature dependence of amino acids directly calculated from protein structures, PLoS Comput. Biol. 11 (2015), e1004277.